Turkish Journal of Earth Sciences

http://journals.tubitak.gov.tr/earth/

Research Article

Turkish J Earth Sci
(2015) 24: 165-178
© TÜBİTAK
doi:10.3906/yer-1404-24

Petrology and geochemistry of mafic dykes from the Muslim Bagh Ophiolite (Pakistan): implications for petrogenesis and emplacement

Mohammad Ishaq KAKAR[1,*], Khalid MAHMOOD[2], Mohammad ARIF[3], Mehrab KHAN[4], Andrew C. KERR[5], Mohibullah MOHIBULLAH[4], Aimal Khan KASI[1]

[1]Centre of Excellence in Mineralogy, University of Balochistan, Quetta, Pakistan
[2]Department of Earth Sciences, University of Sargodha, Sargodha, Pakistan
[3]Department of Geology, University of Peshawar, Peshawar, Pakistan
[4]Department of Geology, University of Balochistan, Quetta, Pakistan
[5]School of Earth and Ocean Sciences, Cardiff University, Cardiff, Wales, UK

Received: 26.04.2014 • **Accepted/ Published Online:** 25.12.2014 • **Printed:** 10.04.2015

Abstract: Two different types of mafic dykes are found in the Muslim Bagh Ophiolite: 1) a sheeted dyke complex and 2) a mafic dyke swarm. Relative to the host plutonic section, the sheeted dykes are poorly developed, implying that they formed in an oceanic setting with a low and intermittent supply of magma, probably because of cyclic accumulation of crystals at the base of the magma chamber. Both the sheeted dykes and the dyke swarms have been metamorphosed to greenschist/amphibolite facies conditions. With the exception of the upper level gabbros and sheeted dykes, the dyke swarms crosscut almost the whole ophiolite suite as well as the metamorphic sole rocks, but are truncated structurally at the contact with the underlying mélange and sediments. Hence, the injection of the dyke swarms postdates the formation of both the main Muslim Bagh Ophiolite and the metamorphic sole rocks, but predates the accretion of the mélange and the final emplacement of the ophiolite onto the Indian plate margin. Both the sheeted dykes and dyke swarms are tholeiitic and have a geochemical signature of either island arc tholeiites (IAT) or are transitional between mid-oceanic ridge basalts and IAT. Oceanic rocks with such characteristics, especially their enrichment in large-ion lithophile elements, are generally thought to have formed by processes involving a subduction zone component in the source region by fluids released from the subducting slab. The Muslim Bagh Ophiolite sheeted dykes originated in the late Cretaceous, in a supra-subduction zone tectonic setting related to the subduction of a narrow branch of the Neo-Tethys Ocean, followed by a subduction rollback due to splitting of the nascent arc in the Tethys Ocean. This intra-oceanic subduction led to the formation of a metamorphic sole, followed by the off-axis intrusion of mafic dykes into the ophiolite through a slab window. The Muslim Bagh Ophiolite was accreted to the Bagh Complex and finally obducted onto the Indian Platform.

Key words: Sheeted dykes, mafic dyke swarm, petrogenesis, supra-subduction zone setting, emplacement, slab window

1. Introduction

Two types of dykes have been identified in the Muslim Bagh Ophiolite: (i) a sheeted dyke complex (dolerite, diorite, and plagiogranite) and (ii) a mafic dyke swarm. Both types occur only in the Saplai Tor Ghar Massif of the Muslim Bagh Ophiolite (Figure 1). Preliminary reports are available on the sheeted dykes, which cut the plutonic crustal section (e.g., Ahmad and Abbas, 1979; Salam and Ahmed, 1986; Sawada et al., 1992; Mahmood et al., 1995; Siddiqui et al., 1996, 2011). Based on the relative time of formation, Sawada et al. (1992) subdivided the sheeted dykes into three types: (a) highly foliated metadolerite, diorite, and plagiogranite, generally metamorphosed and partly mylonitized, (b) weakly foliated metamorphosed amphibolite–greenschist facies, discordant to foliation or layering, and (c) non-foliated and non-metamorphosed, discordant to foliation or layering. Bilgrami (1964) was the first to report the occurrence and briefly describe the mafic dyke swarm. Mahmood et al. (1995) and Siddiqui et al. (1996) subsequently described the field features and petrography of these dykes. The geochemical characteristics of the gabbros from the Muslim Bagh Ophiolite are of island arc tholeiite (IAT) affinity (e.g., Kakar et al., 2013a). Based on a detailed geochemical investigation, the current study aims to determine the magmatic affinity and petrogenesis of the two types of mafic dykes cutting the Muslim Bagh Ophiolite and will discuss the implications of these results for the emplacement mechanism of the ophiolite.

* Correspondence: kakarmi.cemuob@gmail.com

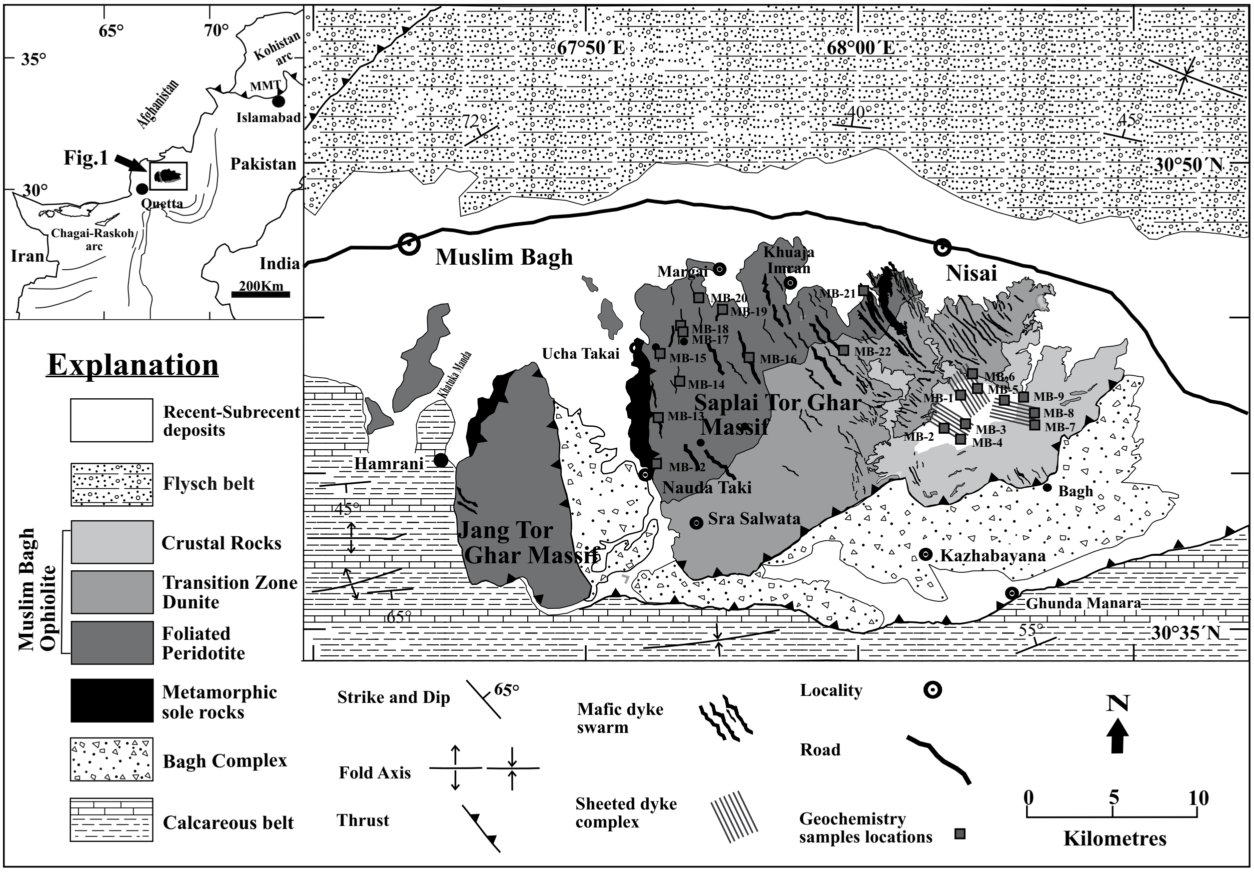

Figure 1. Geological map of the Muslim Bagh area showing the Muslim Bagh Ophiolite, Bagh Complex, the Flysch Belt, and the Calcareous Belt (after Jones, 1961; Van Vloten, 1967; Siddiqui et al., 1996; Kakar et al., 2012).

2. Regional geology and the Muslim Bagh Ophiolite

The rocks in the Muslim Bagh area are divided into three tectono-stratigraphic belts (Figure 1).

1) The tectonically lowermost is the calcareous belt of sediments belonging to the Indian plate passive margin, which are composed of limestone, sandstone, and mudstone ranging in age from early Jurassic to Paleocene (e.g., Jones, 1961; Warraich et al., 1995; Naka et al., 1996; Jadoon and Khurshid, 1996).

2) The calcareous belt is thrust over by the suture zone that consists of the Muslim Bagh Ophiolite and Bagh Complex and lies between the Indian plate and the Afghan block (Gansser, 1964; Jadoon and Khurshid, 1996; Figure 1). The Muslim Bagh Ophiolite is exposed in the form of two major blocks, namely the Jang Tor Ghar Massif (JTGM) and the Saplai Tor Ghar Massif (STGM), that are thrust over a zone of sub-ophiolitic metamorphic rocks and mélange (Bilgrami, 1964; Mahmood et al., 1995; Naka et al., 1996; Figure 1). The ophiolite contains a nearly complete ophiolite sequence, i.e. tectonized peridotite at the base, overlain successively by the mantle–crust transition zone and crustal rocks (e.g., Khan et al., 2007; Figure 1). The metamorphic sole rocks are preserved at the contact with the ophiolitic sequence and can be seen in the northwestern part of the JTGM and the western exposure of the STGM (Kakar et al., 2014a; Figure 1). They mainly consist of basal foliated peridotite and sub-ophiolitic metamorphic rocks that comprise garnet amphibolite facies rocks that grade downwards into amphibolite facies and greenschist facies with calcite–marble inter-layers. The metamorphic sequence also displays decreasing intensity of deformation downward from the stratigraphic base of the ultramafic rocks (e.g., Kakar et al., 2014b). The mantle section of the Muslim Bagh Ophiolite is exposed in both the JTGM and STGM and has a combined thickness of about 11 km (Siddiqui et al., 1996; Figure 1). The serpentinized ultramafic rocks in the mantle section of both massifs consist of foliated peridotite (harzburgite and depleted harzburgite) and dunite, contain segregated bodies of chromite deposits, and are intruded by gabbro and mafic dyke swarms (Kakar et al., 2013b). The mantle section is overlain by a transition zone i.e., several kilometers thick and predominantly consists of dunite with minor amounts of chromite, wehrlite, pyroxenite, and gabbro

as discontinuous bands or lenses (Figure 1). The crustal section of the Muslim Bagh Ophiolite is exposed in the eastern portion of the STGM and is characterized by a sequence of ultramafic–mafic cumulates and a sheeted dyke complex. The former is mainly composed of a single or cyclic repetition of layered dunite, wehrlite, pyroxenite, and gabbro (Kakar et al., 2014c). The sheeted dyke complex consists of dolerites, plagiogranites, and diorites. The gabbroic rocks comprise layered, foliated, and isotropic types (Mahmood et al., 1995). The Muslim Bagh Ophiolite formed 80.2 ± 1.5 Ma ago (Kakar et al., 2012) and was tectonically emplaced about 68.7 ± 1.5 Ma ago (Mahmood et al., 1995). The Bagh Complex consists of igneous and sedimentary rocks bounded by each other with parallel thrusts (Mengal et al., 1994). The geochemical signatures of basalts from the Bagh Complex suggest both normal mid-oceanic ridge basalt (NMORB) and ocean island basalt (OIB) tectonic settings (e.g., Sawada et al., 1992; Kakar et al., 2014c).

3) The Pishin belt (Kasi et al., 2012), also called the Flysch belt (Naka et al., 1996), lies to the north of the suture zone and comprises the Eocene Nisai Formation (Allemann, 1979), the Oligocene Khojak Formation (Qayyum et al., 1996) and the Miocene–Pliocene fluvial successions of the Multana Formation (Jones, 1961) overlain by the Pleistocene lacustrine Bostan Formation (Jones, 1961).

3. Field and petrographic features

3.1. Sheeted dykes

The sheeted dykes crop out within the plutonic crustal section of the eastern segment of the STGM (Figure 1). Field observations reveal that these sheeted dykes are less developed. Some of the dykes display well-developed chilled margins and generally trend between 140° and 160° and dip 55° towards the northeast (Figure 2a). Reconstruction on the basis of structural data on sheeted dykes suggests the paleospreading ridge axis for the Muslim Bagh region was oriented at about 145° (Mahmood et al., 1995). The sheeted dyke complex of the Muslim Bagh Ophiolite is about 1 km thick (Siddiqui et al., 1996), rooted in the gabbroic rocks of the crustal sequence, and appears to have formed in stages by multiple injections of basic and acidic magmas. The sheeted dykes mostly comprise meta-dolerites with inclusions and small dykes of plagiogranites and diorites intruding the middle part of the sheeted dyke complex.

Metamorphosed dolerite dykes consist of hornblende, ferro-hornblende, ferro-actinolite, ferro-tremolite, plagioclase, and minor quartz (Mahmood et al., 1995). The small prismatic euhedral to subhedral crystals of hornblende show chloritization, especially along their margins, and contain magnetite along fractures. The plagioclase ranges from oligoclase to andesine and is mostly interstitial to hornblende. The mostly euhedral to subhedral grains of plagioclase appear dusty because of extensive alteration, namely argillization and sericitization. Some of the plagioclase grains display zoning. Small subhedral to anhedral grains of ilmenite, magnetite, and hematite occur scattered throughout the rock.

3.2. Mafic dyke swarm

The mafic dyke swarm found in the Muslim Bagh Ophiolite crosscut the mantle, lower crustal, and metamorphic sole rocks but did not cut through the upper level gabbros and sheeted dyke complex. They strike 140° to 170° and are abundant in the STGM with a few dykes found on the western side of the JTGM (Figure 1). These dykes range in thickness from 1 to 15 m across and extend up to many kilometers (Figures 2b and 2c). They possess chilled margins and appear to have produced contact metamorphic effects in the adjacent country rocks (Figure 2d). In places, the dykes and the enclosing country rocks are sheared and stretched into boudins. When followed up-sequence, they show a typical gabbroic texture in the center. Locally, the dykes are much more abundant and display spectacular crisscross or anastomosing relationships (Figure 2b). Elsewhere, the dykes are disposed irregularly and comprise alternating widely spaced (5 dykes per km) and closely spaced (15 dykes per km) groups (Bilgrami, 1964). The most closely spaced dykes occur in the northern and northeastern parts of the mantle–crust transition zone (Figure 1).

The dykes in the swarm are mostly doleritic in composition. They are light to dark grey, medium to fine-grained and often exhibit sub-ophitic texture, i.e. grains of clinopyroxene partially enclosing laths of plagioclase (Figure 2e). The preserved primary minerals are clinopyroxene (both augite and pigeonite), plagioclase, and spinel while chlorite, calcite, pectolite, and zeolites are the main secondary phases. In some samples the plagioclase laths are clear (Figure 2e), while in other samples they are almost completely altered to sericite (Figure 2f). Minute flakes of pale brown biotite and fine needles of dark brown amphibole are observed in some of these rocks. Some of the dolerites are very fine grained, display a microcrystalline or micro-ophitic texture, and consist chiefly of clinopyroxene and plagioclase, spinel, and accessory amounts of secondary minerals, e.g., chlorite and zeolite. Veins of calcite or calcite-filled fractures are common. The pyroxene grains are mostly anhedral, show well-developed cleavages, and their form is usually determined by the pattern of the plagioclase laths.

A few of these dykes contain quartz and samples from these quartz-bearing dykes consist mainly of intricate micro-pegmatitic intergrowths of altered plagioclase and quartz, light green chlorite, a few crystals of colorless augite,

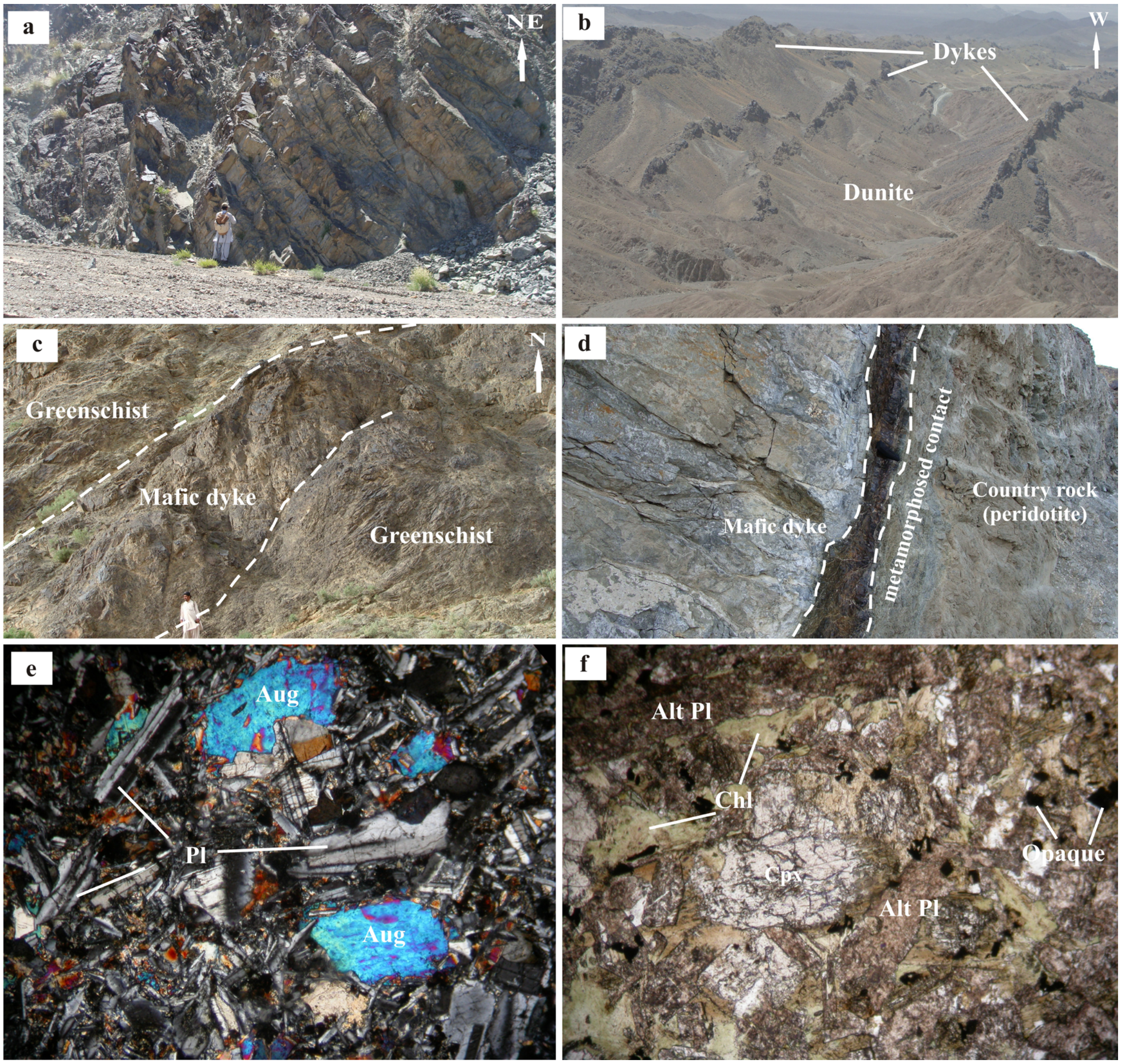

Figure 2. a) Photograph showing the trend of sheeted dykes; b) a view of the mafic dyke swarm looking down a hilltop, Saplai Tor Ghar Massif of the Muslim Bagh Ophiolite; c) a dyke crosscutting a greenschist facies rock near Nauda Taki, Saplai Tor Ghar Massif of the Muslim Bagh Ophiolite; d) a mafic dyke cutting through peridotite exposed in a road cut, Saplai Tor Ghar Massif of the Muslim Bagh Ophiolite; e) photomicrograph (XPL, ×5) showing sub-ophitic texture in dolerite consisting of augite crystals and laths of plagioclase; f) photomicrograph (PPL, ×5) of dolerite from the dyke swarm showing clinopyroxene (Cpx) partially altered to chlorite (Chl) and altered plagioclase (Alt Pl).

coffee brown spinel, and tiny discrete grains of quartz. The micro-pegmatitic intergrowths of quartz and plagioclase are plume-shaped. Some of the dolerite samples consist of euhedral to anhedral crystals of brown hornblende, with rounded grains of clinopyroxene, saussuritized plagioclase, pale green clinozoisite, and anhedral spinel. The hornblende forms rims around the clinopyroxene. The spinel is black and usually forms skeletal crystals enclosing the pyroxene and hornblende.

The alteration in dolerites from the dyke swarm is very pronounced. The plagioclase crystals are extensively altered to sericite so determination of their composition is not possible (Figure 2f). In some specimens, the plagioclase has been saussuritized and replaced by an aggregate of clinozoisite and sericite. Pale green chlorite is the dominant ferromagnesian mineral and has developed at the expense of both the clinopyroxene and hornblende (Figure 2f). The chlorite alteration begins around the grain margins and proceeds inwards along intragranular cracks and cleavages. The hornblende is dark brown and often forms rims around the pyroxene grains. The epidote is colorless to pale yellow and only weakly pleochroic. The spinel shows considerable variation, with magnetite and picotite being the common varieties, though never occurring together in the same rock. The occurrence of spinel as skeletal crystals is very common. Alteration of picotite to chromite is common, and magnetite often shows a dense brown alteration rim, probably of limonite. The modal composition of the dolerite dyke swarm is summarized as plagioclase (55%–75%), pyroxene (15%–30%), opaque (8%), quartz (2%–8%), accessory and secondary products like hornblende (4%–6%), chlorite (1%–2%), and sericite (Bilgrami, 1964).

4. Geochemistry

4.1. Analytical methods

Twenty samples (9 from the sheeted dykes and 11 from the mafic dyke swarm) were analyzed for major and trace elements. Additionally, 3 samples from the sheeted dykes and 4 from the mafic dyke swarm were analyzed for rare earth elements (REEs). The major elements were determined on fused glass beads formed from homogenized mixtures with a sample-to-flux (lithium tetraborate) ratio of 1:5, whereas hydraulically pressed powder pellets were used for trace element analysis. Both the major and trace element analyses were carried out using a Philips Wavelength Dispersive X-Ray Fluorescence Spectrometer (WD/XRF) at the Geoscience Research Laboratories, Geological Survey of Pakistan, Islamabad, Pakistan. Samples for the REE analysis were prepared using a standard Teflon vial acid digestion method using a mixture of HF ± $HClO_4$–HNO_3 and spiked to 50 ng/mL with indium as an internal standard. The REE analyses were calibrated against a set of multi-element working standard solutions and performed using a PerkinElmer ELAN 6100 Inductively Coupled Plasma Mass Spectrometer (ICP-MS) at the Amdel Laboratories, Adelaide, Australia. The analytical data from all of the samples of both the sheeted dykes and mafic dykes swarm are reported in the Table and presented in Figures 3 to 6.

4.2. Classification

There is substantial agreement amongst petrologists and geochemists that the high field strength elements (HFSEs) (Ti, Zr, Y, Nb, Ta, Hf, and Th) and the REEs (La, Ce, Pr, Nd, Sm, Eu, Gd, Tb, Dy, Ho, Er, Tm, Yb, and Lu) are normally immobile during moderate hydrothermal alteration (e.g., Humphris and Thompson, 1978; Staudigel, 2003). As described in the petrology section, both the sheeted dykes and dyke swarm samples are moderately to highly altered. We have chosen the least altered samples for the geochemical analyses and avoided use of the major elements (e.g., SiO_2, K_2O + Na_2O) and mobile trace elements (such as Pb, Ba, Rb, and K) for the purpose of classification and discrimination. Thus, most of the plots used for classification, geochemical discrimination, and interpretation of these dyke samples are based on the HFSEs and REEs.

The samples from the sheeted dykes and dyke swarm are classified on the more alteration-resistant Zr/Ti versus Nb/Y diagram of Pearce (1996). All of the samples of these dykes fall within the basalt field on this diagram (Figure 3a) and both types of dykes show a geochemical affinity with oceanic tholeiites (Figure 3b).

4.3. Major element characteristics

The major elements in the samples from the sheeted dyke complex of the Muslim Bagh Ophiolite display the following variation (wt%): MgO (4.6–7.7), CaO (8.5–12.5), low concentration of TiO_2 (0.5–1.5), Na_2O + K_2O (1.5–4.6), and relatively little variation in the concentration of SiO_2 (48.6–54.2), Al_2O_3 (14.5–18.7), and $Fe_2O_3^t$ (8.5–11.8). Variation in the major element composition of samples representing the mafic dyke swarm is as follows (wt%): moderately high concentration of CaO (6.9–14.3), restricted range of TiO_2 (0.7–1.8), alkalis (Na_2O + K_2O = 4.2–6.9), small but variable amount of MgO (4.3–8.0), relatively uniform Al_2O_3 (14.4–16.0), $Fe_2O_3^t$ (8.2–12.8), and low to moderate SiO_2 content (43.6–50.5). The low contents of TiO_2 and P_2O_5 may be a reflection of the tholeiitic character of the studied samples (Figure 3d). Comparison between the two dyke types reveals that the sheeted dykes contain higher SiO_2 but distinctly lower Na_2O than the samples from the dyke swarm. The variable concentration of CaO and Na_2O + K_2O in the dyke rocks of the Muslim Bagh Ophiolite may be in part due to alteration as indicated by the presence of small veinlets of calcite and epidote.

4.4. Trace element characteristics

The Muslim Bagh sheeted dykes contain higher but variable amounts (ppm) of the large-ion lithophile elements (LILEs) than the MORBs, e.g., Rb (1.5–4.5), Ba (55–277), Sr (178–337), moderate concentrations of most of the HFSEs, Zr (29–89), Y (16–23), Ce (20.2–71.6), but low Nb (1.8–4.2). The samples from the mafic dyke swarm contain more variable and mostly higher amounts (in ppm) of Rb (1.6–30.4), but lesser Ba (32–147) and Ce (11.1–48.6) than the sheeted dykes. While the Zr contents (47–91) of the dyke swarm samples are similar to those of the sheeted dykes, their Sr (88–594) and Y (16–30) concentrations range to higher values than the sheeted dykes. The wider range of CaO content is most probably a result of post-magmatic alteration, which is obvious from the occurrence of calcite and/or epidote veins and fracture-fills and relatively high values for the loss on ignition (LOI) of most of the studied samples. This process may also have remobilized the LILEs (Rb, K, Ba, and Sr) (Humphris and Thompson, 1978; Staudigel, 2003).

The Zr contents are plotted on Harker-type binary diagrams against some of the (i) major and minor element oxides, such as MgO, Al_2O_3, TiO_2, and P_2O_5 and (ii) HFSEs, e.g., Zn, Co, Y, and Nb (Figure 4). While some of the plots

Table. Major oxide (wt%), trace and REE element (ppm) composition of the sheeted dykes and mafic dyke swarm.

Rock type	Sd	Sd	Sd	Sd	Sd	Sd	Sd	Sd	Sd	Ds	Ds	Ds	Ds	Ds	Ds	Ds	Ds	Ds	Ds	Ds
Sample no.	**MB-1**	**MB-2**	**MB-3**	**MB-4**	**MB-5**	**MB-6**	**MB-7**	**MB-8**	**MB-9**	**MB-12**	**MB-13**	**MB-14**	**MB-15**	**MB-16**	**MB-17**	**MB-18**	**MB-19**	**MB-20**	**MB-21**	**MB-22**
SiO_2	52.4	54.21	52.73	52.04	48.61	52.2	52.74	49.83	49	50.18	47.79	45.45	43.58	50.53	49.6	46.12	50.35	49.62	49.43	50.48
TiO_2	1.12	0.93	1.12	0.8	0.52	0.92	0.94	1.45	0.71	0.73	0.8	0.74	1.34	1.51	1.51	0.88	1.09	1.03	1	1.81
Al_2O_3	16.07	15.56	15.5	16.45	18.71	16.17	16.17	14.54	16.04	15.82	15.52	15.98	15.21	14.97	15.19	14.39	15.77	14.88	15.56	14.98
Fe_2O_3	11.62	10.95	11.82	10.03	8.52	9.47	10.56	11.16	10.15	8.99	8.8	8.23	11.57	12.14	11.89	8.93	10.92	10.55	10.46	12.82
MnO	0.23	0.23	0.07	0.2	0.28	0.16	0.21	0.22	0.22	0.19	0.18	0.17	0.22	0.23	0.23	0.19	0.22	0.21	0.2	0.25
MgO	4.85	4.56	5.46	6.1	7.03	6.07	5.31	6.03	7.66	6.98	7.99	7.79	7.75	4.32	4.95	7.93	5.85	5.6	6.91	4.75
CaO	8.72	8.51	8.85	9.59	12.5	9.51	9.45	9.55	11.68	9.46	11.4	10.3	14.28	6.92	7.33	12.17	8.35	11.36	9.49	8.3
Na_2O	3.48	3.51	1.25	3.09	2.28	2.51	3.08	4.36	2.72	4.25	3.46	5.65	5.2	6.1	5.89	6.15	4.88	4.01	3.64	4.42
K_2O	0.43	0.38	0.2	0.42	0.34	0.34	0.57	0.2	0.54	0.21	0.83	1.24	0.07	0.61	0.29	0.28	0.48	0.18	0.82	0.17
P_2O_5	0.18	0.19	0.19	0.14	0.05	0.14	0.19	0.13	0.11	0.1	0.08	0.06	0.11	0.15	0.14	0.09	0.09	0.1	0.07	0.14
LOI	0.91	0.97	2.81	1.14	1.15	2.5	0.78	2.42	1.18	2.19	3.13	4.37	0.67	2.52	2.97	2.87	1.98	2.45	2.43	1.89
Total	**100.01**	**100**	**100**	**100**	**99.99**	**99.99**	**100**	**99.89**	**100.01**	**99.1**	**99.98**	**99.98**	**100**	**100**	**99.99**	**100**	**99.98**	**99.99**	**100.01**	**100.01**
Sc	28.2	29.7	32.2	33.8	36.5	31.7	30	27.1	37.9	33.1	35.9	26.7	30.2	22.3	19.4	39.8	28.1	30.3	27	33.3
V	353.9	288.8	306.5	254.1	206.5	268.7	284.6	234.7	240.2	223.9	216.4	177.7	288	336	301.6	231.1	331.2	292.3	290.4	456.4
Cr	38.5	27.9	18.3	42.2	49.1	18.8	30.7	51.4	109.9	227.1	232.3	190.9	95.9	14.2	58.5	155.5	23.1	22.5	43.2	17.3
Co	57.6	51.7	50.4	56.7	45.8	49.2	54.3	45.6	53.2	51.3	44.8	49.5	50.8	45.7	40.5	45.8	46.4	64.9	53	50.4
Ni	22	12.7	9	22	35	18.5	19.7	32	38.7	46	84.1	66.6	57.5	16	15.5	75	30	25.8	36	14.5
Cu	139	82.4	2.8	68.1	16.6	0.3	111.6	78.4	50.2	67.5	79.8	68.4	124.1	102.5	57.3	74.5	153.8	137.7	135	2.2
Zn	85	68.1	15.5	56.5	61.5	31.5	60.8	90	65.9	60	55.1	49.6	61.7	100	82.8	60	95	57.9	62.8	58.3
Ga	21	30	21	29.9	25.2	26.2	29.1	19.5	27.2	16	24.7	26.2	22.7	19.5	27.3	14.5	18	24.9	27	29.1
As				0.3			0.4			1.6	0.2	0.3		0.5	0.3	1.4	0.3		1.1	
Br	3.4	3.1	2.9	2.8	2.6	2.9	3.5	3.6	2.6	2.9	2.5	2.1	3	3	4.1	1.3	3.5	3	2.7	2.6
Rb	1.7	1.8	1.3	3	3.2	2.6	4.5	1.5	5.9	24.2	16.7	30.4		8.3	2.7	1.8	7.6	1.6	16.5	
Sr	264.3	237.7	254.2	231.8	195.1	336.6	251	177.8	268.2	151.1	594.4	422.2	87.6	157.1	156.8	275	130.5	119.2	210.2	207.5
Y	21.7	20.6	23.3	18.5	11.9	20.3	19.5	27.1	15.6	16.3	17.7	16.8	18.5	29.5	26.4	18.3	19.2	22.3	19.4	26
Zr	76.4	71.1	78.4	66.5	28.9	69.7	69.8	88.9	50.8	46.6	68.4	55.5	46.9	90.6	78.7	52.6	48.5	56.8	51.5	76.3

Table. (Continued).

Nb	3.3	3.1	4.2	3	1.8	3.5	4.1	4	2.4	1.3	1.4	0.7	1.9	3.4	2.8	1.1	1.6	1.9	1.5	2.9
Mo				0.4				0.1						0.6						
Ag	17.9	25.2	19.6	23.5	17.9	19.6	17.3	16.6	22.2	24.4	16	20.2	17.6	24.2	16.1	16.6	18.7	21.2	19.7	20.6
Cd	6.8	14.1	8.4	14.7	6.7	8	9.1	8.6	7.4	0.1	6.2	9.4	8.4	0.1	9.7	6	8	8.1	8.6	11.6
Sn	12.4	16.6	8.1	15.2	11.5	13.7	12.5	14.7	12.7	15.3	9.6	11.2	10.6	13.5	15.7	11.8	10.9	12.2	11.1	10.9
Sb			0.8	2.7	2.1	1.1			3.9		4.2	1.1	1.5		2.4	0.3	2.5	2.8		
Cs	0						3.6			0.7				0.2		1.1	0.9		2	
Ba	121.9	125.1	54.7	105.2	101.1	94.2	159.2	92.8	276.9	136.3	125.1	79	31.6	99.4	57.3	44.7	64.5	59.8	146.5	97.8
La	13.1	17.5	12.3	21.5	7.1	22.8	20.9	9.4	18.4	12.1	9.8	13.7	13.8	14.4	13.2	13.2	7	10.4	5.8	8.9
Ce		71.6	20.2	37.6	30.6	28.7	5	27.6	35.7	23.5	48.6	30.5	25.1	22.3	36.2	25.1	24.3	39	22.8	11.1
Nd	13.5	12.5	12.8	9.1	11.5	11.5	11.7	11.9	4.2	14	12.1	6	12	10.1	13.6	6.3	5.9	7	9.5	
Sm	3.5		3.7			1.9		3.4		2		2.7		3.5		2.1	2.3	28.6		
Yb	2.5		2.4					3.2		1.95				3.5		2.3	2.4			
Hf	27.6	31	25.8	21.1	24.9	38.4	12.5	30.2	18.3	14.1	27.1	27.3	28.8	17.9	22.2	19.7	26.9	3.1	33.7	20.9
Ta	2.6	5.8	7.2		5.1	4	3.2			1.1	3.2	3.2			8.2	0.5		3.1	3.8	
Pb	1.5							1.5		0.5				0.53			0.5			
Bi	16.2	16.3	15.5	16.5	14.6	14.4	18.3	15.3	16.2	14.9	16.6	14.7	16.4	13.3	15.8	14	15.6	16.8	16.1	14.8
Th	2.11	0.17	2.3	0.47	3.34	4.48	7.25	5.41	4	3.8	8.42	2.4	9.1	8.1	2.5	4.1	2.54	6.9	4.7	3.6
Tm	0.35		0.35					0.45		0.25				0.27		0.35	0.35			
Tb	0.62		0.66					0.74		0.42				0.8		0.52	0.54			
Pr	3.1		3.3					2.1		1.25				2		1.25	1.2			
Lu	0.41		0					0.27		0.23				0.4		0.3	0.28			
Ho	0.82		0.88					1.05		0.6				1.1		0.74	0.76			
Gd	3.4		3.6					3.6		2.1				3.9		2.4	2.6			
Eu	1.25		1.2					1.25		0.78				1.15		0.82	0.86			
Er	2.6		2.7					3.2		1.9				3.5		2.3	2.4			
Dy	4.2		4.5					5		3				5.5		3.7	3.8			

Note: LOI = loss on ignition, Fe_2O_3 = total iron, Sd = sheeted dykes, Ds = dyke swarm.

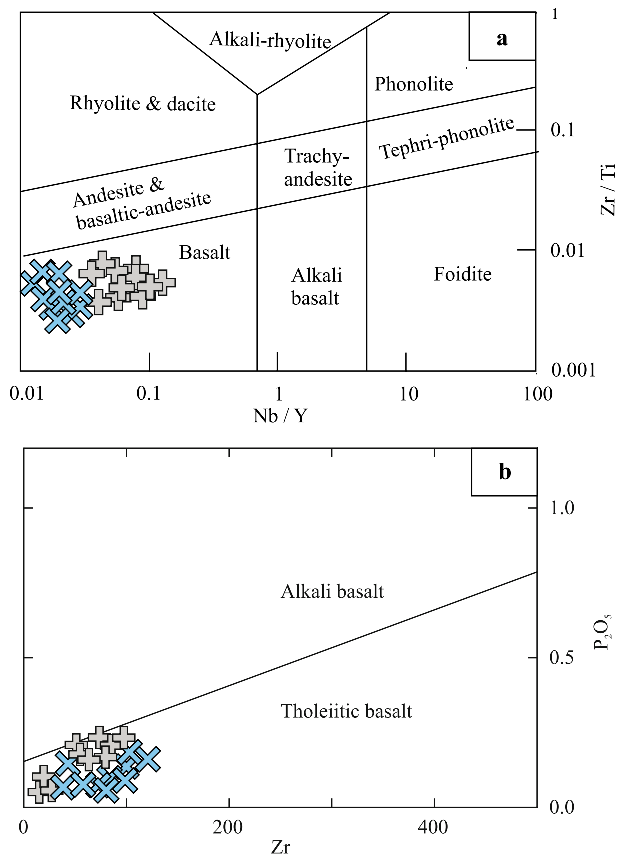

Figure 3. Geochemical characterization of the sheeted dykes (+) and dyke swarm (**X**) from the Muslim Bagh Ophiolite using the discrimination diagrams of (a) Pearce (1996) and (b) Winchester and Floyd (1976).

show a scatter of the data points (e.g., Zr against Zn and Co), others display well-defined fractionation trends. For example, the plots of Zr versus TiO_2, P_2O_5, Y, and Nb display positive trends, while Zr versus MgO shows a negative relationship. The less scattering of data points and systematic inter-element variations indicate that the HFSE are relatively unaffected by secondary alteration.

The trace element data on the sheeted dykes and mafic dyke swarm of the Muslim Bagh Ophiolite were further evaluated through multi-element normalized plots. The NMORB and chondrite-normalized data on the studied samples show flat patterns parallel to NMORB for both the HFSEs and the heavy rare earth elements (HREEs), but enrichment in LILEs and light rare earth elements (LREEs) relative to NMORB (Figure 5). Compared to the sheeted dykes (Figure 5d), the chondrite-normalized REE patterns of the mafic dyke swarm (Figure 5b) are flat to slightly LREE-depleted, with the exception of La and Ce.

5. Discussion

5.1. Petrogenesis of sheeted dykes and mafic dyke swarm

The presence and nature of a sheeted dyke complex in an ophiolite complex implies an approximate balance between spreading rate and magma supply in an extensional setting (Robinson et al., 2008). The sheeted dyke complex of the Muslim Bagh Ophiolite is poorly developed compared to its plutonic section (Figure 1). This particular configuration of the Muslim Bagh Ophiolite crustal sequence suggests that the sheeted dykes formed under conditions of low and discontinuous magma supply (e.g., Cannat et al., 1995) probably because of crystallization of many cycles of cumulates in the magma chamber as plutonic rocks. The total absence or low degree of development of sheeted dyke complex indicates the lack of balance between the rate of spreading and magma supply (Robinson et al., 2008), which is usually the case in supra-subduction zone environments.

The dyke swarms of the Muslim Bagh Ophiolite are mostly dolerites. They crosscut almost the entire ophiolite suite as well as the metamorphic sole rocks (Figures 1 and 2b–c) but are truncated structurally at the contact of the ophiolite with the underlying mélange and the sediments underneath (Figures 1 and 2a–b). This relationship between the dykes and country rocks indicates that the intrusion of the dyke swarms postdates the formation of the Muslim Bagh Ophiolite at a spreading center, initial intra-oceanic detachment, and the formation of sub-ophiolitic metamorphic sole rocks. No age data are available for the dykes; however, their intrusion must have been at a shallow level where the adjacent country rocks were cold enough to be baked, and, as a consequence, the dykes themselves could develop chilled margins. Therefore, the time span between the intrusion of the dykes and the formation of the metamorphic sole rocks may have been very short. For example, this time span is thought to be about 2 Ma in the case of the Tauride belt of Turkey (cf., Parlak et al., 1996; Dilek et al., 1999).

The geochemistry of both the sheeted dykes and the mafic dyke swarm is that of IAT. This IAT signature is evidenced by the higher contents of LILEs and the flat pattern of the HFSEs and REEs, with no depletion in the LREEs (Figure 5). The enrichment of LILEs may be due to either alteration or addition through subducting a slab-derived hydrous component to the melt source region, i.e. a depleted mantle wedge. However, the positive anomaly of Th and negative anomaly of Nb relative to other incompatible elements in the NMORB-normalized plots support the latter possibility (e.g., Wood, 1980; Hofmann, 1997). The flat pattern (Figure 5b) of both the LREEs and the HREEs (with the exception of elements La and Ce) of the dyke swarms suggest derivation from a depleted mantle source.

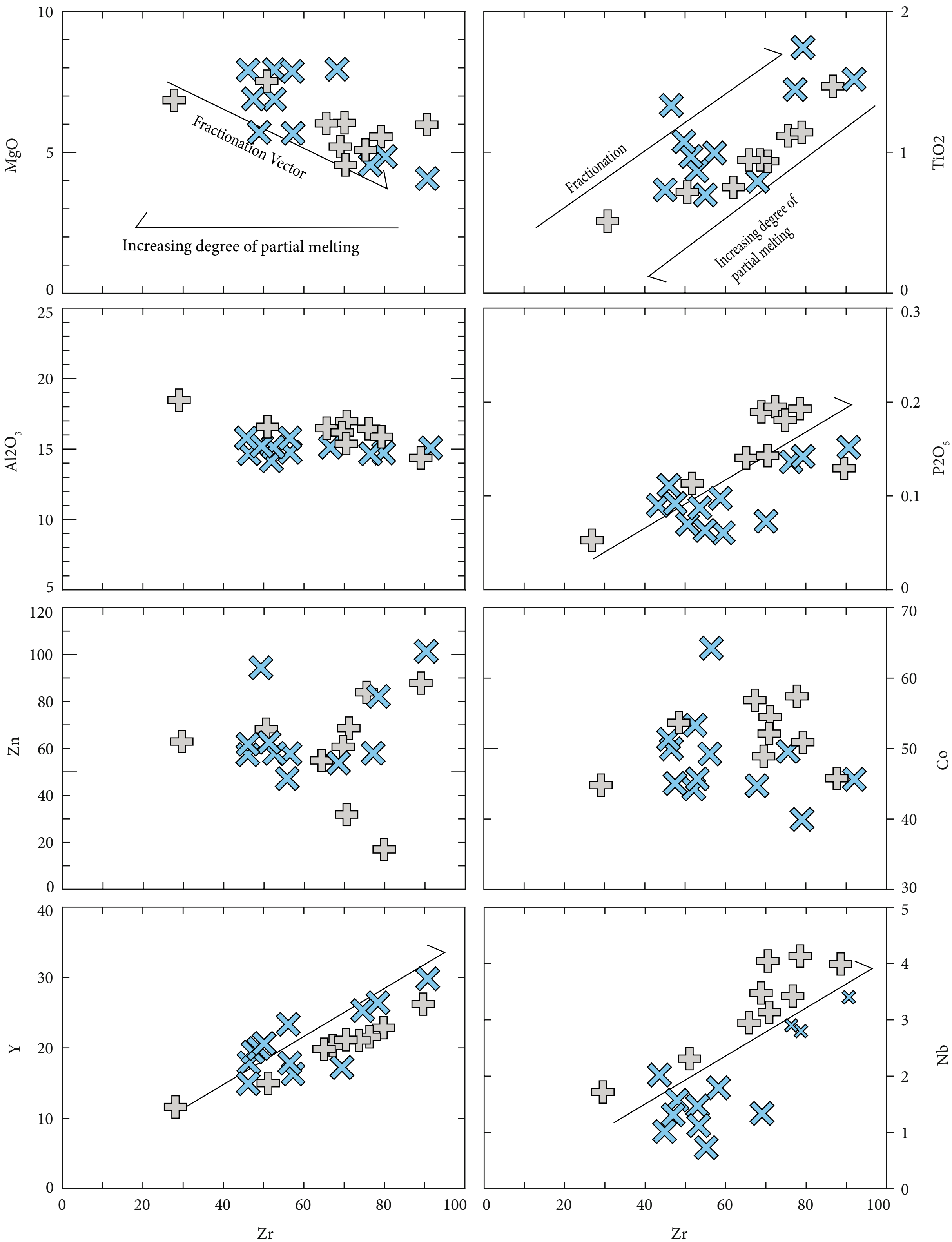

Figure 4. Variation diagrams showing Zr versus selected major element oxides and trace elements for the sheeted dykes (+) and dyke swarm (**X**) from the Muslim Bagh Ophiolite showing distinct fractionation trends.

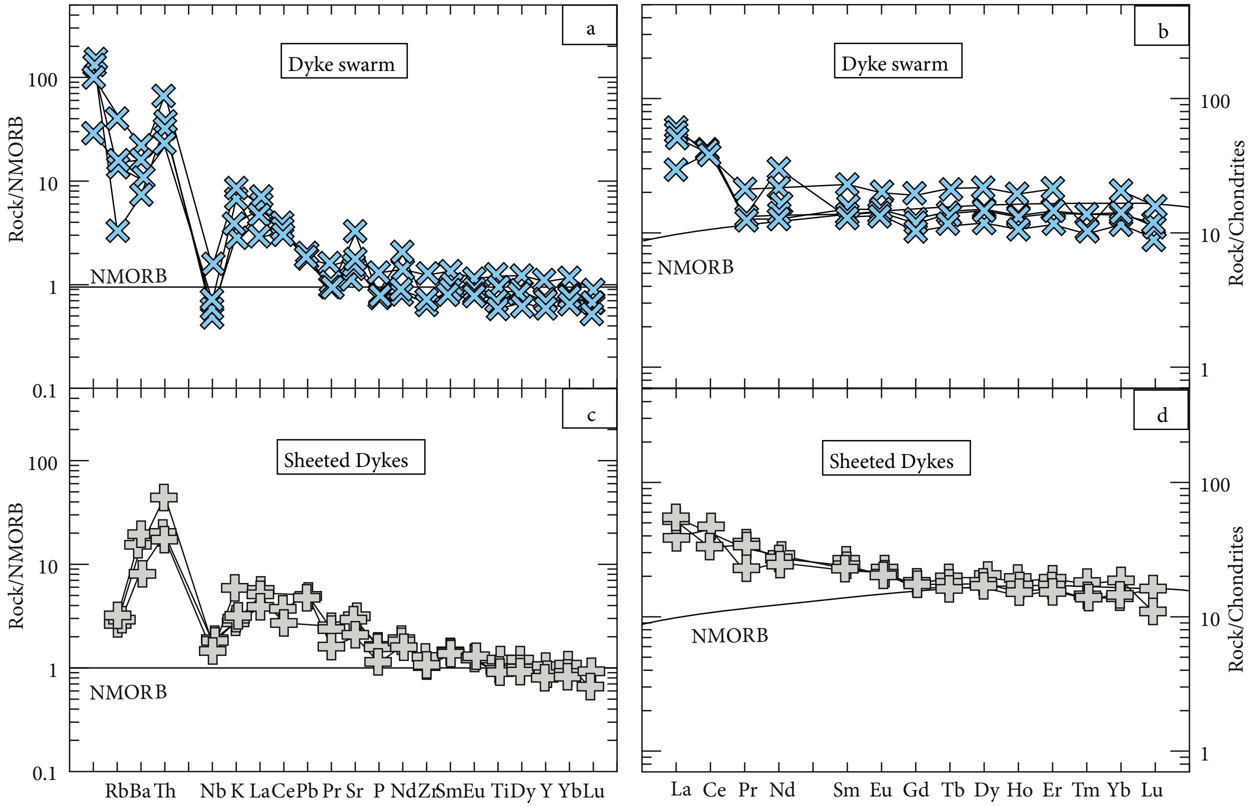

Figure 5. The NMORB and chondrite-normalized plots of the mafic dyke swarm and sheeted dykes from the Muslim Bagh Ophiolite displaying arc-like signatures. See text for details. The values used for normalization are taken from Sun and McDonough (1989).

Weaker subduction signatures coupled with their crosscutting relationship through the mantle peridotite and metamorphic sole rocks suggest that the dyke swarm formed further from the supra-subduction zone, in either space and/or time, than the sheeted dyke complex. A possible model is that the magmas of the dyke swarm formed off-axis and rose through a slab window and may have incorporated a subduction component from the upper asthenosphere (or perhaps the lowermost lithosphere) as they moved upwards. This model can explain the generation and intrusion of the magmas in a compressional setting. The geochemical characteristics of both the sheeted dykes and mafic dyke swarm have a signature of either IAT or are transitional between MORB and IAT (Figure 6). Generally, oceanic rocks exhibiting such characteristics are thought to have formed in a supra-subduction zone tectonic setting (e.g., Pearce and Norry, 1979; Shervais, 1982; Pearce, 2003; Shervais et al., 2004; Robinson et al., 2008).

5.2. Tectonic emplacement model

The Muslim Bagh Ophiolite formed ~80.2 ± 1.5 Ma ago (Kakar et al., 2012) in a supra-subduction zone tectonic setting related to the west–northwest dipping subduction (Gnos et al., 1997) of a narrow branch of the Neo-Tethys Ocean (e.g., Mahmood et al., 1995; Kakar et al., 2014c; Figures 7a and 7b). This was followed by a subduction rollback due to the splitting of the nascent arc in a manner similar to that proposed by Flower and Dilek (2003) and Dilek and Flower (2003). The intra-oceanic subduction led to the formation of a metamorphic sole (Mahmood et al., 1995; Searle et al., 1997; Kakar et al., 2014b) followed by the intrusion of off-axis mafic dykes into both the metamorphic sole and the mantle section of the ophiolite, possibly through a slab/asthenospheric window (Lytwyn and Casey, 1995; Celik, 2007; Figure 7c). The Muslim Bagh Ophiolite continued to accrete the Bagh Complex after the dyke swarm formation and was finally obducted along with the underlying Bagh Complex onto the Indian Platform 50–45Ma ago (cf., Naka et al., 1996; Searle et al., 1997; Zhu et al., 2005; Aitchison et al., 2007; Green et al., 2008; Najman et al., 2010; Figure 7d).

The Muslim Bagh Ophiolite contains two different types of mafic dykes: the sheeted dykes and the dyke swarm. The configuration of a crustal sequence from the Muslim Bagh Ophiolite with a less developed sheeted dyke complex and a thick accumulation of plutonic rocks indicates an imbalance between magma supply and spreading rate in an oceanic environment. Both the sheeted

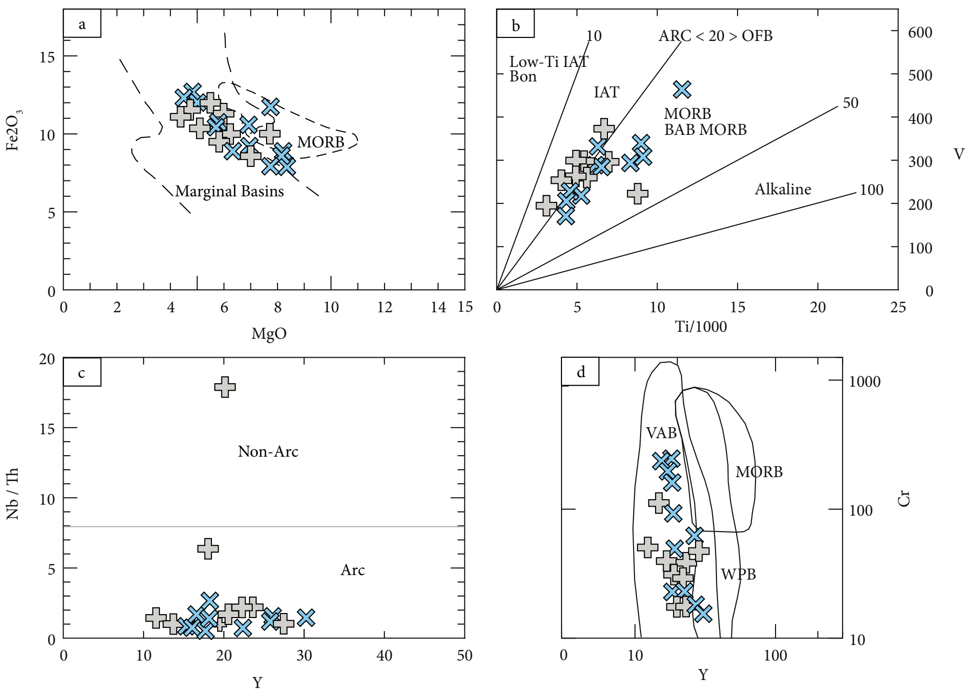

Figure 6. Tectonic discrimination of the sheeted dykes (+) and dyke swarm (**X**) from the Muslim Bagh Ophiolite using diagrams proposed by (a) Saunders and Tarney (1991), (b) Shervais (1982), (c) Jenner et al. (1991), and (d) Pearce (1982).

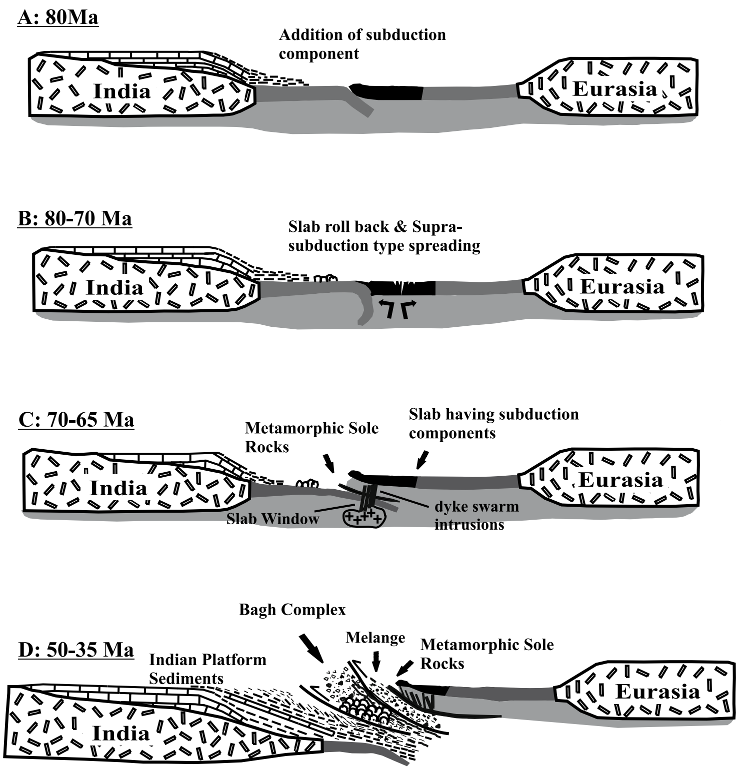

Figure 7. Schematic cross-sections showing the tectonic evolution of the Muslim Bagh Ophiolite Complex and the emplacement of dykes: (A) short-lived subduction and the addition of a subduction component; (B) slab rollback and spreading in the ocean basin and the formation of the Muslim Bagh Ophiolite crust; (C) intra-oceanic subduction, the formation of the metamorphic sole rocks and the subsequent intrusion of the dyke swarm; and (D) final emplacement of the Muslim Bagh Ophiolite and Bagh Complex onto the Indian plate margin.

dykes and mafic dyke swarms were mostly dolerites but were subsequently metamorphosed into greenschist and amphibolite facies assemblages. Mafic dyke swarms crosscut the ophiolite suite and basal metamorphic sole but are structurally truncated at the contact with the underlying mélange. None of these dykes cuts the mélange or platform sediments below the metamorphic sole rocks. Hence, the emplacement/intrusion of the dykes postdated both the formation of the ophiolite and the formation of the metamorphic sole rocks during the initial intra-oceanic subduction, but predated the final emplacement of the ophiolite onto the Indian continent margin. The crosscutting of the dyke swarm through the Muslim Bagh sole rocks indicates that the magma originated below and not above the subduction zone, thus ruling out the mantle wedge and mantle transition zone as sources and indicates that the magma which formed these dykes must have been derived from the spinel peridotite stability zone, i.e. <50–60 km. The geochemical signatures of the sheeted dyke complex and the mafic dyke swarm of the Muslim Bagh Ophiolite have the characteristics of island arc tholeiites consistent with their formation in a supra-subduction zone tectonic setting.

Acknowledgments
This work forms part of the PhD study of the first author. The Higher Education Commission of Pakistan is thanked for funding the geochemical analyses through their programs; Access to Scientific Instrumentation and International Research Support. Osman Parlak, Omer Elitok, and 2 anonymous reviewers are thanked for their review comments that improved the manuscript.

References

Ahmad Z, Abbas SG (1979). The Muslim Bagh Ophiolite. In: Farah A, DeJong KA, editors. Geodynamics of Pakistan. Quetta, Pakistan: Geological Survey of Pakistan, pp. 243–250.

Aitchison JC, Ali JR, Davis AM (2007). When and where did India and Asia collide? J Geophys Res-Sol Ea 112: doi: 10.1029/2006JB004706.

Allemann F (1979). Time of emplacement of the Zhob Valley ophiolites and Bela Ophiolite, Balochistan (preliminary report). In: Farah A, Dejong KA, editors. Geodynamics of Pakistan. Quetta, Pakistan: Geological Survey of Pakistan, pp. 213–242.

Bilgrami SA (1964). Mineralogy and Petrology of the Central Part of the Hindu Bagh Igneous Complex, Hindu Bagh Mining District, Zhob Valley. West Pakistan Geological Survey Records 10.

Cannat M, Karson, JA, Miller, DJ (1995). Proceedings of the Ocean Drilling Program, Initial Reports 153, College Station, TX, USA.

Celik OF (2007). Metamorphic sole rocks and their mafic dykes in the eastern Tauride belt ophiolites (southern Turkey): implications for OIB-type magma generation following slab break-off. Geol Mag 144: 849–866.

Dilek Y, Flower MFJ (2003). Arc-trench rollback and forearc accretion: 2. A model template for ophiolites in Albania, Cyprus, and Oman. In: Dilek Y, Robinson PT, editors. Ophiolites in Earth History. Geol Soc London Spec Publ 218, pp. 43–68.

Dilek Y, Thy P, Hacker B, Grundvig S (1999). Structure and petrology of Tauride ophiolites and mafic dyke intrusions (Turkey): implications for the Neo-Tethyan Ocean. Geol Soc Am Bull 111: 1192–1216.

Flower FJ, Dilek Y (2003). Arc-trench rollback and forearc accretion: 1. A collision-induced mantle flow model for Tethyan ophiolites. In: Dilek Y, Robinson PT, editors. Ophiolites in Earth History. Geol Soc London Spec Publ 218, pp. 21–41.

Gansser A (1964). Geology of the Himalayas. London, UK: Wiley Interscience.

Gnos E, Immenhauser A, Peters TJ (1997). Late Cretaceous/early Tertiary convergence between the Indian and Arabian plates recorded in ophiolites and related sediments. Tectonophys 271: 1–19.

Green OR, Searle MP, Corfield RI, Corfield RM (2008). Cretaceous–Tertiary carbonate platform evolution and the age of the India–Asia collision along the Ladakh Himalaya (Northwest India). T J Geol 116: 331–353.

Hofmann AW (1997). Mantle geochemistry: the message from oceanic volcanism. Nature 385: 219–229.

Humphris SE, Thompson G (1978). Trace element mobility during hydrothermal alteration of oceanic basalts. Geochim Cosmochim Ac 42: 127–136.

Jadoon IAK, Khurshid A (1996). Gravity and tectonic model across the Sulaiman fold belt and the Chaman fault zone in western Pakistan and eastern Afghanistan. Tectonophys 254: 89–109.

Jenner GA, Dunning GR, Malpas J, Brown M, Brace T (1991). Bay of Islands and Little Port complexes, revisited: age, geochemical and isotopic evidence confirm supra-subduction zone origin. Can J Earth Sci 28: 135–162.

Jones AG (1961). Reconnaissance Geology of Part of West Pakistan. A Colombo Plan Cooperative Project. Toronto, Canada: Government of Canada.

Kakar MI, Collins AS, Mahmood K, Foden JD, Khan M (2012). U-Pb zircon crystallization age of the Muslim Bagh Ophiolite: enigmatic remains of an extensive pre-Himalayan arc. Geology 40: 1099–1102.

Kakar MI, Mahmood K, Khan M, Kasi AK, Manan RA (2013a). Petrology and geochemistry of gabbros from the Muslim Bagh Ophiolite: implications for their petrogenesis and tectonic setting. J Himalayan Earth Sci 46: 19–30.

Kakar MI, Mahmood K, Kerr AC, Khan M (2013b). Petrology of the mantle rocks from the Muslim Bagh Ophiolite, Balochistan, Pakistan. J Himalayan Earth Sci 46: 101–112.

Kakar MI, Khan M, Mahmood K, Kerr AC (2014a). Facies and distribution of metamorphic rocks beneath the Muslim Bagh Ophiolite (NW Pakistan): tectonic implications. J Himalayan Earth Sci 47: (in press).

Kakar MI, Mahmood K, Khan M, Plavsa D (2014b). Petrology and geochemistry of amphibolites and greenschists from the metamorphic sole of the Muslim Bagh ophiolite (Pakistan): implications for protolith and ophiolite emplacement. Arab J Geosci: doi 10.1007/s12517-014-1613-6.

Kakar MI, Kerr AC, Collins AS, Mahmood K, Khan M, McDonald I. (2014c). Supra-subduction zone tectonic setting of the Muslim Bagh Ophiolite, northwestern Pakistan: insights from geochemistry and petrology. Lithos 202–203: 190–206.

Kasi AK, Kassi AM, Umar M, Manan RA, Kakar MI (2012). Revised lithostratigraphy and tectonic zones of the Pishin Belt, northwestern Pakistan. J Himalayan Earth Sci 45: 53–65.

Khan M, Kerr AC, Mahmood K (2007). Formation and tectonic evolution of the Cretaceous–Jurassic Muslim Bagh Ophiolitic Complex, Pakistan: implications for the composite tectonic setting of ophiolites. J Asian Earth Sci 31: 112–127.

Lytwyn JN, Casey JF (1995). The geochemistry of post-kinematic mafic dyke swarms and subophiolitic metabasites, Pozanti-Karsanti ophiolite, Turkey: evidence for ridge subduction. Geol Soc Am Bull 107: 830–850.

Mahmood K, Boudier F, Gnos E, Monié P, Nicolas A (1995). 40Ar/39Ar dating of the emplacement of the Muslim Bagh ophiolite, Pakistan. Tectonophys 250: 169–181.

Mengal JM, Kimura K, Siddiqui MRH, Kojima S, Naka T, Bakht MS, and Kamada K (1994). The lithology and structure of a Mesozoic sedimentary–igneous assemblage beneath the Muslim Bagh ophiolite, Northern Balochistan, Pakistan. Bul Geol Surv Japan 5: 51–61.

Najman Y, Appel E, Boudagher-Fadel M, Bown P, Carter A, Garzanti E, Vezzoli G (2010). Timing of India–Asia collision: geological, biostratigraphic, and palaeomagnetic constraints. J Geophys Res-Sol Ea 115: doi: 10.1029/2010JB007673.

Naka T, Kimura K, Mengal JM, Siddiqui RH, Kojima S, Sawada Y (1996). Mesozoic sedimentary-igneous complex, Bagh Complex, in the Muslim Bagh Area, Pakistan. Opening and closing ages of the Ceno-Tetheyan Branch. In: Yajima J, Siddiqui RH, editors. Proceedings of Geoscience Colloquium, Geoscience Laboratory, Geological Survey of Pakistan 16, pp. 47–94.

Nicolas A (1989). Structures of Ophiolites and Dynamics of Oceanic Lithosphere: Dordrecht, Netherlands: Kluwer.

Parlak O, Delaloye M, Bingol E (1996). Obduction direction of the Mersin ophiolite: structural evidence from the subophiolitic metamorphics in the central Taurus Belt, southern Turkey. Int Geol Rev 38: 778–786.

Pearce JA (1982). Trace element characteristics of lavas from destructive plate margins. In: Thorpe RS, editor. Andesites: Orogenic Andesites and Related Rocks. Chichester, UK: Wiley, pp. 525–548.

Pearce JA (1996). A user's guide to basalt discrimination diagrams. In: Wyman DA, editor. Trace Element Geochemistry of Volcanic Rocks: Applications for Massive-sulphide Exploration. Geological Association Canada Short Course Notes12, pp. 79–113.

Pearce JA (2003). Supra-subduction zone ophiolites: the search for modern analogues. In: Dilek Y, Newcomb S, editors. Ophiolite Concept and the Evolution of Geological Thought. Geol Soc Am Spec Publ 373, pp. 269–294.

Pearce JA, Norry ML (1979). Petrogenetic implications of Ti, Zr, Y, and Nb variations in volcanic rocks. Contrib Mineral Petr 69: 33–47.

Qayyum M, Niem AR, Lawrence RD (1996). Newly discovered Paleogene deltaic sequence in Katawaz basin, Pakistan and its tectonic implications. Geology 24: 835–838.

Robinson PT, Malpas J, Dilek Y, Zhou M-F (2008). The significance of sheeted dyke complexes in ophiolites. GSA Today 18: 4–10.

Salam A, Ahmed Z (1986). Ophiolitic ultramafic-mafic rocks from Bagh area: Zhob District, Pakistan. Acta Mineralogica Pakistanica 2: 65–73.

Saunders AD, Tarney J (1991). Back-arc basins. In: Floyd P, editor. Ocean Basalts. London, UK: Blackie, pp. 219–263.

Sawada Y, Siddiqui RH, Khan SR, Aziz A (1992). Mesozoic igneous activity in the Muslim Bagh area, Pakistan, with special reference to hotspot magmatism related to the break-up of the Gondwanaland: In: Proceedings of Geoscience Colloquium Geoscience Laboratory, Geological Survey of Pakistan 1, pp. 21–70.

Searle M, Corfield RI, Stephenson B, McCarron J (1997). Structure of the north Indian continental margin in the Ladakh-Zanskar Himalayas: implications for the timing of obduction of the Spontang ophiolite, India–Asia collision and deformation events in the Himalaya. Geol Mag 134: 297–316.

Shervais JW (1982). Ti-V plots and the petrogenesis of modern and ophiolitic lavas. Earth Planet Sci Lett 59: 101–118.

Shervais JW, Kimbrough DL, Renne P, Hanan B, Murchey B, Snow CA (2004). Multi-stage origin of the coast range ophiolite, California: implications for the life cycle of supra-subduction zone ophiolites. Int Geol Rev 46: 289–315.

Siddiqui RH, Aziz A, Mengal JM, Hoshino K, Sawada Y (1996). Geology, petrochemistry and tectonic evolution of Muslim Bagh Ophiolite Complex Balochistan, Pakistan. Geologica 3: 11–46.

Siddiqui RH, Mengal JM, Hoshino K, Sawada Y, Brohi IA (2011). Back-arc basin signatures represented by the sheeted dykes from the Muslim Bagh Ophiolite Complex, Balochistan, Pakistan. SURJ 43: 51–62.

Staudigel H (2003). Hydrothermal alteration processes in the oceanic crust. In: Holland HD, Turekian KK, editors. Treatise on Geochemistry, Vol. 3. 1st ed. Elsevier, pp. 511–535.

Sun SS, McDonough WF (1989). Chemical and isotopic systematics of oceanic basalts: implications for mantle composition and processes. In: Saunders AD, Norry MJ, editors. Magmatism in the Ocean Basins. Geol Soc London Spec Publ 42, pp. 313–345.

Van Vloten R (1967). Geology and Chromite Deposits of the Nisai area, Hindu Bagh Mining District, West Pakistan. Geological Survey of Pakistan 2.

Warraich MY, Ali M, Ahmed MN, Siddiqui MRH (1995). Geology and structure of the calcareous zone in the Muslim Bagh in the Qilla Saifullah area, Balochistan. Geologica 1: 61-75.

Winchester JA, Floyd PAF (1976). Geochemical magma type discrimination: application to altered and metamorphosed igneous rocks. Earth Planet Sci Lett 28: 459–469.

Wood DA (1980). The application of a Th–Hf–Ta diagram to problems of tectono-magmatic classification and to establishing the nature of crustal contamination of basaltic lavas of the British tertiary volcanic province. Earth Planet Sci Lett 50:11–30.

Zhu B, Kidd WS, Rowley DB, Currie BS, Shafique N (2005). Age of initiation of the India-Asia collision in the east-central Himalaya. J Petrol 113: 265–285.